Lawrence Berkeley Laboratory
UNIVERSITY OF CALIFORNIA

Materials & Molecular Research Division

To be published in the ACS Symposium Series on
"The Chemistry of Lanthanides and Actinides"
American Chemical Society Meeting, Washington, DC
September 10-15, 1979

SPECIFIC SEQUESTERING AGENTS FOR THE ACTINIDES

Kenneth N. Raymond, William L. Smith, Frederick L. Weitl,
Patricia W. Durbin, E. Sarah Jones, Kamal Abu-Dari,
Stephen R. Sofen and Stephen R. Cooper

September 1979

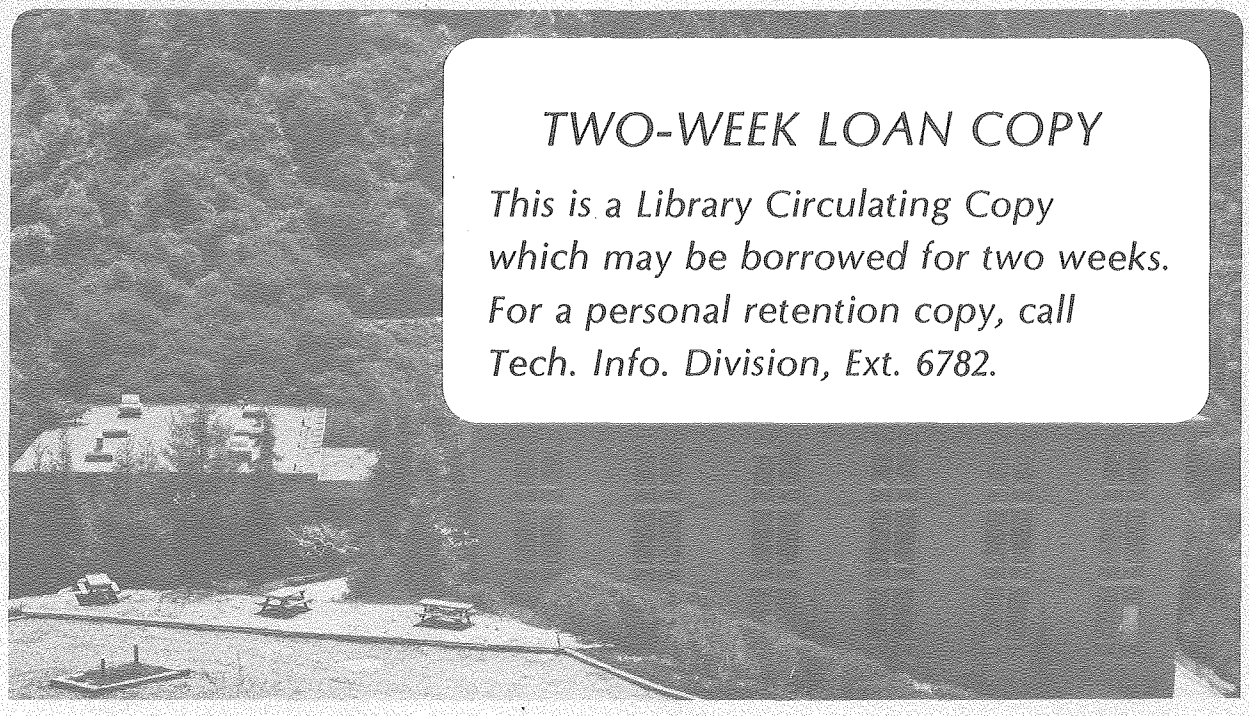

Prepared for the U.S. Department of Energy under Contract W-7405-ENG-48

DISCLAIMER

LBL-10327

Specific Sequestering Agents for the Actinides

Kenneth N. Raymond,* William L. Smith, Frederick L. Weitl, Patrica W. Durbin, E. Sarah Jones, Kamal Abu-Dari, Stephen R. Sofen and Stephen R. Cooper

Department of Chemistry

University of California

Berkeley, California 94720

and

Divisions of Materials and Molecular Research, and Biology and Medicine

Lawrence Berkeley Laboratory

Berkeley, California 94720

*Address correspondence to this author at the Department of Chemistry, University of California

Abstract

This paper summarizes the current status of a continuing project directed toward the synthesis and characterization of chelating agents which are specific for actinide ions — especially Pu(IV) — using a biomimetic approach that relies on the observation that Pu(IV) and Fe(III) has marked similarities that include their biological transport and distribution in mammals. Since the naturally-occurring Fe(III) sequestering agents produced by microbes commonly contain hydroxamate and catecholate functional groups, these groups should complex the actinides very strongly and macrocyclic ligands incorporating these moieties are being prepared. We have reported the isolation and structure analysis of an isostructural series of tetrakis(catecholato) complexes with the general stoichiometry $Na_4[M(C_6H_4O_2)_4]\cdot 21\ H_2O$ (M = Th, U, Ce, Hf). These complexes are structural archetypes for the cavity that must be formed if an actinide-specific sequestering agent is to conform ideally to the coordination requirements of the central metal ion. The $[M(cat)_4]^{4-}$ complexes have the D_{2d} symmetry of the trigonal-faced dodecahedron. The complexes $Th[RC(O)N(O)R]_4$ have been prepared where R = isopropyl and R' = t-butyl or neopentyl. The neopentyl derivative is also relatively close to an idealized D_{2d} dodecahedron, while the sterically more hindered ~~isopropyl~~ t-butyl compound is distorted toward a cubic geometry. The synthesis of a series of 2,3-dihydroxy-benzoyl amide derivatives of linear and cyclic tetraaza- and diazaalkanes is reported. Sulfonation of these compounds improves the metal complexation and *in vivo* removal of plutonium from test animals. These results substantially exceed the capabilities of compounds presently used for the therapeutic treatment of actinide contamination.

With the commercial development of nuclear reactors, the actinides have become important industrial elements. A major concern of the nuclear industry is the biological hazard associated with nuclear fuels and their wastes.[1,2] In addition to their chemical toxicity, the high specific activity of alpha emission exhibited by the common isotopes of the transuranium elements make these elements potent carcinogens.[3-7] Unlike organic poisons, biological systems are unable to detoxify metal ions by metabolic degradation. Instead, unwanted metal ions are excreted or immobilized.[8] Unfortunately, only a small portion of absorbed tetra- or trivalent actinide is eliminated from a mammalian body during its lifetime. The remaining actinide is distributed throughout the body but is especially found fixed in the liver and in the skeleton.[5,7,9-12] While the ability of some metals to do damage is greatly reduced by immobilization, local hot spots of radioactivity are produced by immobilized actinides thereby increasing their carcinogenic properties. Thus removal of the actinides from the body is required therapy for actinide contamination.

Conventional chelating agents as diethylenetriaminepentaacetic acid, DTPA (Figure 1), remove much of the soluble actinide present in body fluids, but are almost totally ineffective in removing the actinide after it has left the circulating system or after hydrolysis of the metal to form colloids and polymers.[13-15] The inability of DTPA to completely coordinate the tetravalent actinides is shown by the easy formation of ternary complexes between Th(DTPA) and many bidentate ligands.[16-18] The hydrolysis of Th(IV) and U(IV) DTPA complexes at pH near 8 is explained by the dissociation of H^+ from a coordinated water molecule.[19-22] In addition, the polyaminocarboxylic acids are toxic due

to the indiscriminate complexation and removal of many metals of biological importance, primarily calcium and zinc.[23-26] Thus there is a need for the development of powerful chelating agents highly specific for tetravalent actinides, particularly plutonium(IV).

While not the most toxic, plutonium is the most likely transuranium element to be encountered. Plutonium commonly exists in aqueous solution in each of the oxidation states from III to VI. However, redox potentials, complexation, and hydrolysis under biological conditions strongly favor Pu(IV) as the dominant species.[27,28] It is remarkable that there are many similarities between Pu(IV) and Fe(III) (Table 1). These range from the similar charge per ionic-radius ratios for Fe(III) and Pu(IV) (4.6 and 4.2 e/Å respectively) and their formation of highly insoluble hydroxides to their similar transport properties in mammals. The majority of soluble Pu(IV) present in body fluids is rapidly bound by the iron transport protein transferrin at the site which normally binds Fe(III). In cells, deposited plutonium is initially bound to the iron storage protein ferritin and eventually becomes associated with hemosiderin and other long term iron storage proteins.[9,29,30] These similarities of Pu(IV) and Fe(III) suggest to us a biomimetic approach to the design of Pu(IV) sequestering agents modeled after the very efficient and highly specific iron sequestering agents, siderophores, which were developed by bacteria and other microorganisms for obtaining Fe(III) from the environment.[31-33]

The siderophores (Figure 2) typically contain hydroxamate or catecholate functional groups which are arranged to form an octahedral cavity the exact size of a ferric ion. Catechol, 2,3-dihydroxybenzene,

and the hydroxamic acids, N-hydroxyamides, are very weak acids that ionize to form "hard" oxygen anions, which bind strongly to strong Lewis acids such as Fe(III) and Pu(IV). Complexation by these groups forms five-membered chelate rings, which substantially increases the stability compared to complexation by lone oxygen anions.[34] That the hydroxamic acids strongly coordinate tetravalent actinides is supported by the formation constants presented in Table 2. Due to its higher charge and stronger basicity, the catecholate group is expected to form stronger complexes with the tetravalent actinides than the hydroxamic acids. Thus our goal has been the incorporation of hydroxamate or catecholate functional groups into multidentate chelating agents that specifically encapsulate tetravalent actinides.

The similarity between Fe(III) and the actinide(IV) ions ends with their coordination numbers. Because of the larger ionic radii of the actinide ions, their preferred coordination number found in complexes with bidentate chelating agents is eight. Occasionally higher coordination numbers are encountered with very small ligands or by the incorporation of a solvent molecule.[41,42] Theoretical calculations indicate that either the square antiprism (D_{4d}) or the trigonal faced dodecahedron (D_{2d}) is the expected geometry for an eight coordinate complex. The coulombic energy differences between these polyhedra (Figure 3) is very small and the preferred geometry is largely determined by steric requirements and ligand field effects. Cubic coordination lies at higher energy, but may be stabilized if f-orbital interactions were important. Another important eight coordinate polyhedron, the bicapped trigonal prism (C_{2v}), corresponds to an energy minimum along the transformation pathway between the square antiprism and the

dodecahedron.[43-48] As seen in Table 3, all four of the above geometries are found in eight coordinate complexes of tetravalent actinides with bidentate ligands. However, the mmmm isomer of the trigonal faced dodecahedron is the most prevalent in the solid state.

Actinide Catecholates

A fundamental question in the design of an actinide specific sequestering agent is the coordination number and geometry actually preferred by the metal ion with a given ligand. The complexes formed by Th(IV) or U(IV) and catechol, in which the steric restraints of a macrochelate are absent, serve as structural archetypes for designing the optimum actinide(IV) sequestering agent. Thus the structures of an isoelectronic, isomorphous series of tetrakis-catecholato salts, $Na_4[M(C_6H_4O_2)_4]\cdot 21H_2O$; M = Th(IV), U(IV), Ce(IV), and Hf(IV), were determined by single crystal X-ray diffraction. Suitable crystals were isolated from the reaction of the metal chlorides or nitrates and the disodium salt of catechol in aqueous solution under an inert atmosphere.[64,65] Measurement of magnetic susceptibility and electronic spectra of the cerium and uranium complexes verified the presence of the +4 oxidation state.

It was somewhat surprising that the strongly oxidizing Ce(IV) ion (E_o = +1.70 V)[66] did not react with the catechol dianion, a facile reducing agent.[67] The ability of catechol to coordinate without reduction of oxidizing ions as Ce(IV), Fe(III),[68] V(V),[69] and Mn(III)[70] is a reflection of its impressive coordinating ability. The Ce(IV) complex was found by cyclic voltammetry to undergo a quasi-reversible one-

electron reduction in strongly basic solution in the presence of excess catechol (Figure 4). Using the Nernst equation[71] and the measured potential of the Ce(IV)/(III)(catechol)$_4$ couple of -448 mV vs. NHE, the formation constant of the tetrakis Ce(IV) complex was found to be greater than the corresponding Ce(III) complex by a factor of 10^{36}, consistent with the more acidic character of Ce(IV). This enormous shift of the redox potential of the Ce(IV)/Ce(III) couple is dramatic evidence of the enormous affinity of the catecholate anion for the tetravalent lanthanides and actinides.

The crystal structure of this isostructural series of catechol complexes consists of discrete $[M(catechol)_4]^{4-}$ dodecahedra, a hydrogen bonded network of 21 waters of crystallization and sodium ions, each of which is bonded to two catecholate oxygens and four water oxygens. Of the possible eight coordinate polyhedra, only the cube and the dodecahedron allow the presence of the crystallographic $\bar{4}$ axis on which the metal ion sits. As depicted in Figure 5 and verified by the shape parameters in Table 4, the tetrakis(catecholato) complexes nearly display the ideal D_{2d} molecular symmetry of the mmmm isomer of the trigonal-faced dodecahedron.

The symmetry of the dodecahedron, which can be regarded as the intersection of one elongated and one compressed tetrahedron, allows for different M-O_A and M-O_B bond lengths. As seen in Table 5, the experimental M-O bond lengths are equal in the thorium and cerium complexes. However, the M-O_B bond length is significantly shorter than the M-O_A bond length in the uranium and hafnium complexes. The much smaller ionic radius of the hafnium pulls the catecholate ligands in

sufficiently so that interligand contacts become significant; the short oxygen-oxygen distance between A sites of 2.550 Å, nearly 0.3 Å less than that for the cerium salt, is well within the van der Waals contact distance of 2.8 Å.[73] This lengthens the $M-O_A$ bond of the hafnium complex relative to the others. However, since the ionic radius of uranium lies between those of cerium and thorium it is unlikely that the metal size explains the distortion in the uranium complex. As all four complexes are identical in all respects except for the metal ion, the lengthening of the $M-O_A$ bond in the uranium complex is attributed to a ligand field effect from the f-electrons. A ligand field of D_{2d} symmetry will split the $^3H_4$ ground term for the $5f^2$ configuration of U(IV) into seven levels, two of which are doubly degenerate. The observed temperature-independent magnetic susceptibility of 870 X 10^{-6} cgs mol^{-1} is consistent with a nondegenerate ground state.[74] A qualitative crystal field treatment of the D_{2d} complex predicts a nondegenerate ground state arising from either the f_{xyz} or f_{z^3} metal orbital. Thus from electron repulsion arguments, one expects the ligand oxygen that is closer to the z axis, O_A, to interact more with the filled metal orbital resulting in the observed lengthening of the $M-O_A$ bond.

Actinide Hydroxamates

As with the actinide catecholates, we are interested in determining the optimum structure of actinide hydroxamates for use in the design of an octadentate actinide sequestering agent. Thus the structures of tetrakis(N-isopropyl-3,3-dimethylbutano- and -2,2-dimethylpropano)-hydroxamatothorium(IV) have been determined by single crystal X-ray diffraction.[75] Keeping the pH as low as possible, these compounds

precipitate upon the addition of an aqueous solution of thorium tetrachloride to an aqueous solution of the sodium salt of the hydroxamic acid. The analogous uranium(IV) complexes were prepared similarly under an inert atmosphere using deaerated solvents. Crystals of Th(i-Pr-N(O)-C(O)-t-Bu)$_4$ were obtained by slow evaporation of an ether-hexane solution, while the more soluble Th(i-Pr-N(O)-C(O)-Neopentyl)$_4$ was crystallized by slow evaporation from hexane. Only one set of signals, which were slightly shifted from the uncomplexed ligand, were observed in the room-temperature ^{1}H-nmr spectra of these complexes in chloroform solution, establishing the presence of a single isomer or a fluxional molecule. In the presence of excess ligand, an average signal was observed, indicative of rapid ligand exchange. In addition to their hydrocarbon solubility, the bulky alkyl substituents impart other interesting properties to these complexes. They melt at 127-8 and 116-7 $^{\circ}$C and, under a vacuum of 10^{-3} torr, sublime at 95 and 100 $^{\circ}$C, respectively.

The alkyl substituents are also very important in determining the structures of the thorium hydroxamates. As with the tetracatecholates, the metal ion in the t-Bu complex sits on a crystallographic $\bar{4}$ axis limiting the possible eight coordinate polyhedra to the dodecahedron and the cube (or tetragonal prism). In order to minimize steric interactions, the t-butyl groups situate themselves on the corner of a tetrahedron, resulting in the distorted cubic geometry of the complex shown in Figure 6. This steric strain also manifests itself in the C(=O)-C(t-Bu) bond length of 1.547(5) Å, which is significantly longer than 1.506(5) Å, the length normally found for an sp^2-sp^3 C-C bond.[76] Because the hydroxamate anion is an unsymmetrical ligand with most of

the charge localized on the nitrogen oxygen, the Th-O_N bond, 2.357(3) Å, is 0.14 Å shorter than the Th-O_C bond, 2.492(3) Å. The average Th-O bond, 2.425 Å, is very close to the average Th-O bond found in $[Th(catechol)_4]^{4-}$, 2.420 Å. The O_N-M-O_C (or bite) angle observed in the t-Bu complex of 62.32(9)° is smaller than the value required to successfully span an edge of a cube, 70.53°, calculated using a hard-sphere model. The disparity in Th-O bond lengths and observed bite angle cause a distortion towards the gggg-isomer of a trigonal faced dodecahedron accompanied by a 10.3° twist in the BAAB trapezoid (see Figure 4 for these definitions). As expected theoretically[43,44], the more negatively charged nitrogen oxygens are located at the B sites of the dodecahedron, but this could also be a steric effect of the t-butyl groups.

The relationship of the cube and the dodecahedron to the coordination polyhedron of the t-Bu complex is shown in Figure 7 and a detailed shape parameter analysis is presented in Table 6. The similarity of this complex to a cube is shown by the equal edge lengths of those not spanned by the ligands, the m and g′ edges, and the dihedral angles, δ, which are close to 90° about the m and g edges. The a and b edges are face diagonals in the cube and the dihedral angles about these edges measure the distortion towards the dodecahedron. Although molecular orbital calculations based on electronic repulsions in eight-coordinate complexes favor the dodecahedron, steric repulsions are expected to dominate,[43,44] and the bulky alkyl substituents direct the geometry of the complex towards a cube. In addition, since only one hydroxamate oxygen is charged, the electronic repulsions are diminished. Because the ligands span alternate edges of two parallel square faces, the [illegible] is best designated as the ssss isomer of a cube (after the designations

for a square-antiprism made by Hoard and Silverton[43]) with the overall symmetry of the S_4 point group.

The influence of the t-butyl group in determining structure is greatly reduced by the introduction of a methylene group between the carbonyl carbon and the t-butyl group. Contrary to the previous complex, the neopentyl complex crystallizes in a triclinic space group with 1/2 molecule of hexane per thorium. The structure shown in Figures 8 and 9, is close to the mmmm-dodecahedron found in the tetrakis-(catecholato)thorium and the majority of other eight-coordinate actinide complexes with bidentate ligands (Table 3). While the lack of crystallographic symmetry would allow structures other than the dodecahedron such as the square antiprism or bicapped trigonal prism, the smallest dihedral angle is 35.5° which precludes the presence of any square faces in the coordination polyhedron (for which $\delta = 0$). As seen in Table 6 the complex is, however, distorted from an ideal dodecahedron. The bite of the ligands, which governs the length of the m edges, is smaller than the length of an ideal dodecahedral m edge. This results in the flattening of the B tetrahedron as evidenced by the increased angle between the Th-O_B vector and the pseudo $\bar{4}$ axis, Θ_B, and by the lengthened g edges. The bending of the ligands seen in Figure 8 is due to steric interactions of molecular packing. As before, the Th-O_N bond (ave = 2.36(2) Å), is shorter than the Th-O_C bond (ave = 2.46(4) Å). There is no site preference for the charged oxygen as the O_N and O_C are equally distributed over the A and B sites of the dodecahedron, resulting in a mmmm-dodecahedron with C_1 symmetry.

The coordination chemistry of uranium(IV) with hydroxamic acids is

complicated by the existence of the stable uranyl ion. Uranium tetrachloride is quantitatively oxidized via an oxygen transfer reaction with two equivalents of N-phenylbenzohydroxamic acid anion (PBHA) in tetrahydrofuran (THF) to form an uranyl complex and benzanilide.[77] When four equivalents of PBHA were used in the reaction, crystals of $UO_2Cl(PBHA)(THF)_2$ were isolated. With a larger excess of PBHA, a bis hydroxamate complex was formed. The structure of $UO_2Cl(PBHA)(THF)_2$, shown in Figure 10, was determined by X-ray diffraction. The linear uranyl ion has an average U-O distance of 1.75(3) Å, and is surrounded by a planar pentagonal array composed of two hydroxamate oxygen atoms, a chloride ion and two THF oxygens, such that the chloride ion is opposite the hydroxamate group. The distances from the uranium atom to the charged hydroxamate oxygens (ave = 2.35(3) Å) are slightly shorter than to the THF oxygens (ave = 2.45(3) Å). The U-Cl bond length is 2.68(1) Å.

Substituents are known to be important in determining the redox behavior of hydroxamic acids,[78-82] thus their effect on the oxidation of uranium(IV) was investigated. Reaction of UCl_4 with benzohydroxamic acid anion leads to the formation of tetrakis(benzohydroxamato)-uranium(IV) as the major product. However, this compound undergoes the internal redox reaction upon heating to form an uranyl compound and benzamide. There was no evidence of oxidation-reduction in the synthesis of the tetrakis alkylhydroxamates described above, and only slight decomposition occured on heating. The internal redox reaction displayed by the hydroxamate and uranium(IV) ions is a chemical limitation upon the use of hydroxamate groups in an actinide specific sequestering agent. However this may be avoided by the proper choice of substituent

groups.

Actinide Sequestering Agents

The structures determined for the actinide(IV) catecholates and hydroxamates, as well as with most other ligands, indicate that the mmmm-isomer of the dodecahedron is the preferred geometry. For maximum stability and specificity this geometry should be achieved by the ligating groups of an optimized sequestering agent that encapsulates the tetravalent actinide in a cavity with a radius near 2.4 Å. Molecular models showed that this could be accomplished by the attachment of four 2,3-dihydroxybenzoic acid groups to the nitrogens of a series of cyclic tetraamines via amide linkages as shown schematically in Figure 11. The size of the cavity formed is controlled by the ring size of the tetraazacycloalkane backbone such that a 16 membered ring appeared most promising for the actinides. Two tetra-catechol chelating agents were synthesized, as shown in Figure 12, by the reaction of 2,3-dioxomethylene- or 2,3-dimethoxybenzoyl chloride with 1,4,8,11-tetraazacyclotetradecane or 1,5,9,13-tetraazacyclohexadecane followed by the deprotection of the hydroxyl groups with BBr_3/CH_2Cl_2.[83] Subsequent biological evaluation in mice showed that these compounds reduced the deposition of plutonium into bone and liver. However, they were unable to maintain complexation of the actinide at low pH and released the plutonium in the animals' kidneys.[84] Titrimetric studies of these ligands with tetravalent actinides showed that while they strongly complex actinides, simple one-to-one complexes are not formed at or below neutral pH.

The performance of a ligand at low pH can be improved by increasing

its acidity, thus reducing the competition with protons. The acidity of the catechol groups can be increased by the introduction of strongly electron withdrawing groups on the benzene rings. A more acidic analog of the above ligands was prepared from 2,3-dimethoxy-5-nitrobenzoic acid and 1,4,8,11-tetraazacyclotetradecane. The nitro groups converted the ligand into a deadly liver poison and substantially changed its solubility characteristics such that a large amount of plutonium was found in the soft tissues of the injected mice.[84] In sharp contrast, sulfonation improved the water solubility, stability to air oxidation and the affinity for actinide(IV) ions at low pH. Each 2,3-dihydroxybenzoyl group in the ligands prepared above was monosulfonated regiospecifically at the 5 position by direct reaction with 20-30% SO_3 in H_2SO_4 at room temperature.[85] The increased acidity of the sulfonated derivatives prevented the deposition of plutonium in the kidneys of mice without any appreciable toxic affects.[84]

In order to examine the effect of greater stereochemical freedom, some tetra-2,3-dihydroxy-5-sulfobenzoyl derivatives of linear tetraamines, also shown in Figure 12, have been prepared by similar methods.[85] Maximum stability and specificity towards the actinides, can be obtained by optimizing the length of the methylene bridges between the amine functionalities. Butylene bridges between the nitrogens of the linear tetraamines gave better in vivo results than ethylene or propylene bridges. Biological studies show that the linear derivatives are significantly more effective than the cyclic catechoylamides for actinide removal from mice.[84] In accordance with the trans configuration of amine hydrogens found in the structure of 1,5,9,13-tetraazacyclohexadecane,[86] adjacent catechoylamide groups are expected to lie on opposite

sides of the macrocycle. While inversion about amides is well known, it may not be rapid enough in these compounds to enable coordination of the actinide by all four catechol groups. This is supported by titrimetric data and the fact that the di-2,3-dihydroxy-5-sulfobenzoyldiazaalkanes and the cyclic derivatives are equally effective in plutonium removal from mice.

The catechoylamides were evaluated by the intraperitoneal administration to mice (20 to 30 μmole/kg) 1 hour after the injection of 1.5 μCi/kg of ^{238}Pu(IV) citrate.[84] The mice were killed by cervical dislocation 24 hours after the plutonium injection. The effectiveness of the ligands were ascertained by measuring the plutonium in tissues and excreta using L X-rays, and the results are presented in Table 7. The 4,4,4- or 3,4,3-LICAMS were the most efficient of the catechoylamides tested, each eliminating about 65% of the injected plutonium from the rodents. In addition to sequestering the plutonium from body fluids, skeletal plutonium was reduced to 22% of the control value at the time of ligand injection by 3,4,3-LICAMS. Monomeric dimethyl-2,3-dihydroxy-5-sulfobenzamide, DiMeCAMS, and 2,3-dihydroxybenzoic acid removed very little if any plutonium. Similar results for 2,3-dihydroxybenzoyl-N-glycine were obtained by Bulman and coworkers.[87]

This dramatic difference between the monomeric catechols and the synthetic tetracatechol compounds confirm our original design concept that a macrochelate would be effective biologically in Pu removal. Of the sulfonated catechoylamides only the 4,4,4-LICAMS showed any toxic effects in mice. For comparison, DTPA, the most effective conventional chelating agent, was examined and found to remove 63% of the injected

plutonium. However, the dose-response curve, Figure 13, shows that 3,4,3-LICAMS is much more effective than DTPA at lower doses - up to a two order of magnitude difference.[88] This is a good indication that endogenous metals are not strongly bound by 3,4,3-LICAMS, while metals as calcium and zinc bind strongly to DTPA, reducing the amount of ligand available to complex plutonium. Thus a much larger amount of DTPA is required to achieve the same effective concentration of a smaller quantity of 3,4,3-LICAMS.

The greater efficacy of plutonium decorporation by 3,4,3-LICAMS compared to DTPA has also been observed in beagles.[89] Beagles were treated with a single intravenous injection of 30 μmole/kg of either Ca-DTPA or 3,4,3-LICAMS or 30 μmole/kg of both 30 minutes after an intravenous injection of 0.233 μCi ^{239}Pu(IV), 0.087 μCi ^{237}Pu(IV) and 0.575 μCi ^{241}Am(III) in a citrate buffer. Retention of the radionuclides was determined seven days after their injection. Serious toxic effects were seen in the kidneys of all dogs treated with 3,4,3-LICAMS. The dose response curve of Figure 13 would suggest that smaller doses should be nearly as effective, and may avoid all toxic effects. As seen in Table 8, 3,4,3-LICAMS removed about 86% of the injected plutonium, much better than the 70% removed by DTPA. In contrast, DTPA was much more effective in americium decorporation. This is expected since the affinity of catechol ligands for Ln(III) or An(III) ions is quite low. The measured ratio of the tetrakis(catecholato)Ce(IV)/Ce(III) formation constants of 10^{36} is an indication of the decreased affinity of 3,4,3-LICAMS for the trivalent actinides.[65]

Summary

For the first time a class of sequestering agents has been designed and synthesized for the specific role of complexing plutonium and other actinide(IV) ions. This has resulted from the combination of two observations: (1) That Pu(IV) and Fe(III) are similar in many respects and that this similarity extends to the biological transport and distribution properties of Pu(IV), which accounts for much of the biological hazard of this element. (2) That the design of specific sequestering agents for Fe(III) was solved by microbes a few billion years ago with the production of low molecular-weight chelating agents (siderophores) that incorporate chelating groups such as hydroxamic acids and catechol. The synthetic macrochelates are designed such that the chelating groups can form a cavity that gives eight coordination about the metal and the dodecahedral geometry observed in the unconstrained actinide complexes composed of monomeric ligands. The most promising actinide sequestering agents yet prepared (Table 9) are the sulfonated catechoylamide derivatives of linear tetraamines. These compounds appear to strongly bind tetravalent actinides, while only weak complexation of trivalent and divalent metals has been observed. A derivative of the natural product spermine, 3,4,3-LICAMS, is the most effective in plutonium removal at lower dose concentrations than any other sequestering agent tested to date.

Acknowledgment

This work was supported by the Division of Nuclear Sciences, Office of Basic Energy Sciences, U.S. Department of Energy under Contract No. W-7405-Eng-48.

Literature Cited

1. Blomeke, J. O.; Nichols, J. P.; Mclain, W. C. Physics Today August 1973, 26, 36-42.

2. Kube, A. S.; Rose, D. J. Science 1973, 182, 1205-11.

3. Bienvenu, P.; Nofre, C.; Cier, A. C. R. Acad. Sci. 1963, 256, 1043-4.

4. Stannard, J. N. In, "The Health Effects of Plutonium and Radium"; Jee, W. S. S., Ed.; J. W. Press: Salt Lake City, 1976; pp 363-72.

5. Durbin, P. W. In, "Handbook of Experimental Pharmacology, Vol. 36: Uranium, Plutonium, Transplutonic Elements"; Hodge, H. C.; Stannard, J. N.; Hursh, J. B., Eds.; Springer-Verlag: New York, 1973; pp 739-896.

6. Denham, D. H. Health Physics 1969, 16, 475-87.

7. Bair, J. C.; Thompson, R. C. Science 1974, 183, 715-22.

8. Jones, M. M.; Pratt, T. H. J. Chem. Ed. 1976, 53 342-7.

9. Durbin, P. W. Health Physics 1975, 29, 495-510.

10. International Commission on Radiological Protection, Publication 19: "The Metabolism of Compounds of Plutonium and Other Actinides"; Pergamon Press: New York, 1972.

11. Rundo, J.; Starzyk, P. M.; Sedlet, J.; Larsen, R. P.; Oldham, R. D.; Robinson, J. J. In, "Diagnosis and Treatment of Incorporated Radionuclides"; International Atomic Energy Agency: Vienna, 1976; pp 15-23.

12. Vaughan, J.; Bleany, B.; Taylor, D. M. In, "Handbook of Experimental Pharmacology, Vol. 36: Uranium, Plutonium, Transplutonic Elements"; Hodge, H. C.; Stannard, J. N.; Hursh, J. B., Eds.; Springer-Verlag: New York, 1973; pp 349-502.

13. Catsch, A. In, "Diagnosis and Treatment of Incorporated Radionuclides"; International Atomic Energy Agency: Vienna, 1976; pp 295-305.

14. Smith, V. H. Health Physics 1972, 22, 765-78.

15. Catsch, A.; Harmuth-Hoene, A-E. Biochemical Pharmacology 1975, 24, 1557-62.

16. Pachauri, O. P.; Tandon, J. P. J. Inorg. Nucl. Chem. 1975, 37, 2321-3.

17. Pachauri, O. P.; Tandon, J. P. Indian J. Chem. 1977, 15A, 57-8.

18. Pachauri, O. P.; Tandon, J. P. J. Gen. Chem. USSR (Engl. Transl.) 1977, 47, 398-401; Zh. Obshch. Khim. 1977, 47, 433-6.

19. Carey, G. H.; Martell, A. E. J. Am. Chem. Soc. 1968, 90, 32-8.

20. Bogucki, R. F.; Martell, A. E. J. Am. Chem. Soc. 1958, 80, 4170-4.

21. Fried, A. R.; Martell, A. E. J. Am. Chem. Soc. 1971, 93, 4695-700.

22. Grimes, J. H. In, "Diagnosis and Treatment of Incorporated Radionuclides"; International Atomic Energy Agency: Vienna, 1976; pp 419-60.

23. Cohen, N.; Guilmette, R. Bioinorganic Chem. 1976, 5, 203-10.

24. Sevens, M. J. In, "Metal-Binding in Medicine"; Seven, M. J.; Johnson, L. A., Eds.; J. B. Lippincott: Philadelphia, 1960; pp 95-103.

25. Foreman, H.; Nigrovic, V. In, "Diagnosis and Treatment of Deposited Radionuclides"; Kornberg, H. A.; Norwood, W. D., Eds.; Excerpta Media Foundation: Amsterdam, 1968; pp 419-23.

26. Planas-Bohne, F.; Lohbreier, J. In, "Diagnosis and Treatment of Incorporated Radionuclides"; International Atomic Energy Agency: Vienna, 1976; pp 505-15.

27. Taylor, D. M. In, "Handbook of Experimental Pharmacology, Vol. 36: Uranium, Plutonium, Transplutonic Elements"; Hodge, H. C.; Stannard, J. N.; Hursh, J. B., Eds.; Springer-Verlag: New York, 1973; pp 323-47.

28. Bulman, R. A. Structure and Bonding 1978, 34. 39-77.

29. Taylor, D. M. Health Physics 1972, 22, 575-81.

30. Popplewell, D. S. In, "Diagnosis and Treatment of Incorporated Radionuclides"; International Atomic Energy Agency: Vienna, 1976; pp 25-34.

31. "Microbial Iorn Metabolism"; Nielands, J. B., Ed.; Academic Press: New York, 1974.

32. Raymond, K. N. In, "Advances in Chemistry Series, No. 162: Bioinorganic Chemistry-II"; Raymond, K. N., Ed.; American Chemical Society: Washington, D. C., 1977; pp 33-54.

33. Raymond, K. N.; Carrano, C. J. Accounts Chem. Res. 1979, 12, 183-90.

34. Huhey, J. E. "Inorganic Chemistry: Principles of Structure and Reactivity"; Harper and Row: New York, 1972; pp 418-22.

35. Barocas, A.; Baroncelli, F.; Biondi, G. B.; Grossi, G. J. Inorg. Nucl. Chem. 1966, 28, 2961-7.

36. Dyrssen, D. Acta Chem. Scand. 1956, 10, 353-9.

37. Reidel, A. J. Radioanal. Chem. 1973, 13, 125-34.

38. Zharovskii, F. G.; Ostrovskaya, M. S.; Sukhomlin, R. I. Izv. Vyssh. Ucheb. Zaved., Khim. Khim. Teknol. 1967, 10, 989-93; Chem. Abstr. 1968, 69, 30696y.

39. Chimutova, M. K.; Zolotov, Yu A. Soviet Radiochem. (Engl. Transl.) 1964, 6, 625-30; Radiokhimiya 1964, 6, 640-5.

40. Zharovskii, F. G.; Sukhomlin, R. I.; Ostrovskaya, M. S. Russ. J. Inorg. Chem. (Engl. Transl.) 1967, 12, 1306-9; Zh. Neorg. Khim. 1967, 12, 2476-80.

41. Casellato, U.; Vidali, M.; Vigato, P.A. Inorg. Chim. Acta 1976, 18, 77-112.

42. Moseley, P. T. In, "MTP Int. Rev. Sci.: Inorg. Chem., Ser. Two"; Bagnall, K. W., Ed.; Butterworth: London, 1975; Vol. 7, pp 65-110.

43. Hoard, J. L.; Silverton, J. V. Inorg. Chem. 1963, 2, 235-43.

44. Burdett, J. K.; Hoffmann, R.; Fay, R. C. Inorg. Chem. 1978, 17, 2553-68.

45. Blight, D. G.; Kepert, D. L. Inorg. Chem. 1972, 11, 1556-61.

46. Porai-Koshits, M. A.; Aslanov, L. A. J. Struct. Chem. USSR (Engl. Transl.) 1972, 13, 244-53; Zh. Strukt. Khim. 1972. 13, 266-76.

47. Muetterties, E. L.; Guggenberger, L. J. J. Am. Chem. Soc. 1974, 96, 1748-56.

48. Kepert, D. L. Prog. Inorg. Chem. 1978, 24, 179-249.

49. Allard, B. J. Inorg. Nucl. Chem. 1976, 38, 2109-15.

50. Steffen, W. L.; Fay, R. C. Inorg. Chem. 1978, 17, 779-82.

51. Lenner, M. Acta Crystallogr., Sect. B 1978, 34, 3770-2.

52. Piero, G. D.; Perego, G.; Zazzetta, A.; Brandi, G. Cryst. Struct. Comm. 1975, 4, 521-6.

53. Brown, D.; Holah, D. G.; Rickard, C. E. F. J. Chem. Soc., Sect. A 1970, 423-5.

54. Brown, D.; Holah, D. G.; Rickard, C. E. F. J. Chem. Soc., Sect. A 1970, 786-90.

55. Day, V. W.; Fay, R. C. "Abstracts of Papers", American Crystallographic Association Summer Meeting 1976, p 78.

56. Burns, J. H.; Danford, M. D. Inorg. Chem. 1969, 8, 1780-4.

57. Volz, K.; Zalkin, A.; Templeton, D. H. Inorg. Chem. 1976, 15, 1827-31.

58. Hill, R. J.; Rickard, C. E. F. J. Inorg. Nucl. Chem. 1977, 39, 1593-6.

59. Lenner, M.; Lindquist, O. Acta Crystallogr., Sect. B 1979, 35, 600-3.

60. Baskin, Y.; Prasad, N. S. K. J. Inorg. Nucl. Chem. 1963, 25, 1011-9.

61. Wolf, L.; Bärnighausen, H. Acta Crystallogr. 1960, 13, 778-85.

62. Wessels, G. F. S.; Leipoldt, J. G.; Bok, L. D. C. Z. Anorg. Allg. Chem. 1972, 393, 284-94.

63. Hambley, T. W.; Kepert, D. L.; Raston, C. L.; White, A. H. Aust. J. Chem. 1978, 31, 2635-40.

64. Sofen, S. R.; Abu-Dari, K.; Freyberg, D. P.; Raymond, K. N. J. Am. Chem. Soc. 1978, 100, 7882-7.

65. Sofen, S. R.; Cooper, S. R.; Raymond, K. N. Inorg. Chem. 1979, 18, 1611-6.

66. Latimer, W. M. "Oxidation States of the Elements and Their Potentials in Aqueous Solution", 2nd ed.; Prentice-Hall: Englewood Cliffs, N. J., 1952; p 294.

67. Ho, T.-L.; Hall,T. W.; Wong, C. M. Chem. Ind. (London) 1972, 729-30.

68. Raymond, K. N.; Isied, S. S.; Brown, L. D.; Fronczek, F. F.; Nibert, J. H. J. Am. Chem. Soc. 1976, 98, 1767-74.

69. Cooper, S. R.; Freyberg, D. P.; Raymond, K. N., manuscript in preparation.

70. Magers, K. D.; Smith, C. G.; Sawyer, D. T. Inorg. Chem. 1978, 17, 515-23.

71. Meites, L. "Polarographic Techniques"; Wiley: New York, 1965; p 279.

72. Shannon, R. D. Acta Crystallogr., Sect. A 1976, 32, 751-67.

73. Pauling, L. "The Nature of the Chemical Bond", 3rd ed.; Cornell University Press: Ithica, N. Y., 1960; p 260.

74. Figgis, B. N. "Introduction to Ligand Fields"; Interscience: New York, 1966.

75. Smith, W. L.; Raymond, K. N., manuscript in preparation.

76. "Tables of Interatomic Distances and Configurations in Molecules and Ions, Chem. Soc., Spec. Publ., No. 18, Suppl. 1956-1959"; The Chemical Society: London, 1965.

77. Smith, W. L.; Raymond, K. N. J. Inorg. Nucl. Chem., in press.

78. Minor, D. F.; Waters, W. A.; Ramsbottom, J. V. J. Chem. Soc., Sect B 1967, 180-4.

79. Mackor, A.; Wajer, Th., A. J. W.; de Borer, Th. J. Tetrahedron 1968, 24, 1623-31.

80. Rawson, G.; Engberts, J. B. F. N. Tetrahedron 1970, 26, 5653-64.

81. Ozaki, S.; Masui, M. Chem Pharm. Bull. 1977, 25, 1179-85.

82. Balaban, A. T.; Pascaru, I.; Cuiban, F. J. Mag. Res. 1972, 7, 241-6.

83. Weitl, F. L.; Raymond, K. N.; Smith, W. L.; Howard, T. R. J. Am. Chem. Soc. 1978, 100, 1170-2.

84. Durbin, P. W.; Jones, E. S.; Raymond, K. N.; Weitl, F. L. Radiat. Res., in press.

85. Weitl, F. L.; Raymond, K. N., submitted for publication in J. Am. Chem. Soc.

86. Smith, W. L.; Ekstrand, J. D.; Raymond, K. N. J. Am. Chem. Soc. 1978, 100, 3539-44.

87. Bulman, R. A.; Griffin, R. J.; Russel, A. T., NRPB Report RANDD-1, 1977, 87-9.

88. Durbin, P. W.; Jones, E. S.; Raymond, K. N.; Weitl, F. L., manuscript in preparation.

89. Bruenger, F. W.; Atherton, D. R.; Jones, C. W.; Weitl, F. L.; Durbin, P. W.; Raymond, K. N.; Taylor, G. N.; Stevens, W.; Mays, C. W., manuscript in preparation.

90. Stover, B. J.; Atherton, D. R.; Bruenger, F. W.; Buster, D. S. Health Physics 1968, 14, 193-7.

91. Stover, B. J.; Atherton, D. R.; Buster, D. S. Health Physics 1971, 20, 369-74.

92. Stover, B. J.; Atherton, D. R.; Buster, D. S. In, "The Radiobiology of Plutonium"; Stover, B. J.; Jee, W. S. S., Eds.; J. W. Press: Salt Lake City, 1972; pp 149-69.

Table 1. Similarities of Pu^{4+} and Fe^{3+}.

$\frac{\text{Charge}}{\text{Ionic radius}}$	Pu^{4+}; $\frac{4}{0.96} = 4.2$	Fe^{3+}; $\frac{3}{0.65} = 4.6$
$Fe(OH_3) \rightarrow Fe^{3+} + 3OH^-$		$K \simeq 10^{-38}$
$Fe^{3+} + H_2O \rightarrow Fe(OH)^{2+} + H^+$		$K = 0.0009$
$Pu(OH_4) \rightarrow Pu^{4+} + 4OH^-$		$K \simeq 10^{-55}$
$Pu^{4+} + H_2O \rightarrow Pu(OH)^{3+} + H^+$		$K = 0.031$ (in $HClO_4$)

Pu^{4+} is transported in the blood plasma of mammals as a complex of transferrin, the normal Fe^{3+} transport agent. The Pu^{4+} binds at the same site as Fe^{3+}.

Table 2. Formation Constants for Some Actinide(IV) Hydroxamates.

Metal	Temp, °C	log β_1	log β_2	log β_3	log β_4	Reference
benzohydroxamic acid, Ph-C(O)-N(OH)-H						
U(IV)	25	9.89	18.00	26.32	32.94	35
Th(IV)	25	9.60	19.81	28.76		35
Pu(IV)	25	12.73				35
N-phenylbenzohydroxamic acid, Ph-C(O)-N(OH)-Ph						
Th(IV)	20				37.70	38
Th(IV)	25				37.80	36
Th(IV)	30				37.76	37
Pu(IV)	22	11.50	21.95	31.81	41.35	39
N-phenylcinnamohydroxamic acid, Ph-C=C-C(O)-N(OH)-Ph						
Th(IV)	20	12.76	24.70	35.72	45.72	40

[a] $\log\beta_n = [ML_n]/[M][L]^n$ for the reaction $M^{4+} + nL^- \rightarrow ML_n^{(4-n)+}$

Table 3. Geometry of Monomeric Eight-Coordinate Actinide Complexes with Bidentate Ligands.

Complex	Metals	Idealized Geometry	Ref.
α-M(IV)(acetylacetonate)$_4$	Th,U,Ce	$h_1h_1p_2p_2$-BTP	49,50
β-M(IV)(acetylacetonate)$_4$	Th,U,Np,Ce	ssss-SA	49,51
M(bipyridyl)$_4$	U	ssss-Cube	52
M(IV)(dibenzoylmethanate)$_4$	Th,U,Ce	mmmm-DD	61
M(IV)(N,N-diethyldithiocarbamate)$_4$	Th	mmmm-DD	50,53
[M(III)(N,N-diethyldithiocarbamate)$_4$]$^-$	Np	mmmm-DD	54
M(IV)(diisobutrylmethanate)$_4$	U	BTP	55
M(IV)(hexafluoroacetonylpyrazolide)$_4$	Th,U	mmmm-DD	57
[M(III)(hexafluoroacetylacetonate)$_4$]$^-$	Am,Y,Eu	gggg-DD	56
M(IV)(salicylaldehydate)$_4$	Th,U	mmmm-DD	58
M(IV)(thenoyltrifluoroacetylacetonate)$_4$	Th,U,Pu,Ce	mmmm-DD	59,60

[a] BTP = bicapped trigonal prism, DD = trigonal faced dodecahedron, SA = square antiprism. The isomer notation is taken from references 43 and 46 and corresponds to the edges labelled in Figure 3.

[b] Thorium(trifluoroacetylacetonate)$_4$ was originally described as a 1111-SA (ref. 62), but a reinvestigation established the presence of a coordinated water molecule forming a nine-coordinate complex (ref. 63).

Table 4. Shape Parameters[a] (deg.) for $[M(O_2C_6H_4)_4]^{4-}$, M = Hf, Ce, U, Th, Complexes.

Metal	Θ_A	Θ_B	ϕ	δ
Th	37.9	75.4	3.6	31.3
U	37.1	75.2	3.0	31.1
Ce	36.8	74.9	2.1	32.0
Hf	35.2	73.3	0.4	32.2
Dodecahedron[b]	36.9	69.5	0.0	29.5
Cube[b]	54.7	54.7	0.0	0.0

[a] See references 43 and 47 for definitions of shape parameters.

[b] Calculated using the Hard Sphere Model.

Table 5. Structural Parameters for $Na_4[M(O_2C_6H_4)_4]\cdot 21H_2O$ Complexes.

Metal	Ionic Radius,[a] Å	M-O_A, Å	M-O_B, Å	O_A-O_A, Å	O_A-M-O_B, deg
Th	1.05	2.421(3)	2.418(3)	2.972(6)	66.8(1)
U	1.00	2.389(4)	2.362(4)	2.883(7)	67.7(1)
Ce	0.97	2.362(4)	2.357(4)	2.831(7)	68.3(1)
Hf	0.83	2.220(3)	2.194(3)	2.554(5)	71.5(1)

[a]Reference 72.

Table 6. Shape Parameters[a] for $Th(i\text{-}Pr\text{-}N(O)\text{-}C(O)\text{-}R)_4$.

Parameter	R = t-Butyl[b]	R = Neopentyl	Dodecahedron[c]	Cube[c]
ϕ	10.3	1.1,10.1	0.0	0.0
δ_a	33.2	67.6,70.2	51.3	0.0
δ_b	11.3	35.5,36.5,41.5,48.4	29.5	0.0
δ_g	80.5	42.3,45.4,46.9,51.0 54.0,55.6,58.9,62.7	62.5	90.0
$\delta_{g'}$	69.3		62.5	90.0
δ_m	87.9	70.2,76.2,79.7,85.5	51.3	90.0
Θ_A	44.5	32.9,33.6,35.3,38.8	36.9	54.7
Θ_B	60.0	78.8,82.4,84.0,84.4	69.5	54.7
$M\text{-}O_A/r$[d]	1.06	0.96,0.97,0.99,1.02	1.00	1.00
a/r	1.48	1.11,1.16	1.20	1.63
b/r	1.58	1.32,1.36,1.41,1.60	1.50	1.63
g/r	1.07	1.23,1.27,1.29,1.32 1.34,1.37,1.39,1.40	1.20	1.16
g′/r	1.26		1.20	1.16
m/r	1.27	1.03,1.04,1.04,1.04	1.20	1.16

[a]The shape parameters are defined in references 43 and 47; ϕ is the twist in the BAAB trapezoid, Θ is the angle between the M-O vector and the principal axis, δ_{edge} is the dihedral angle between the faces containing the edge as labeled in Figure 3.

[b]The dodecahedral g edges are divided into edges spanned by the ligands and those which are not, designated g and g′ respectively.

[c]Calculated using the Hard Sphere Model.

[d]r = average $M\text{-}O_B$ distance.

Table 7. Effect of Tetrameric Catechoylamides on the Distribution of $^{238}Pu(IV)$ in Mice.[a]

Compound	Percent Absorbed Dose[b]					
	Liver	Skeleton	Soft Tissue	GI Tract	Kidneys	Whole Body
3,4,3-LICAMS	22(9)	7(1)	1.8(3)	3.3	1.2	35.4
4,4,4-LICAMS	25(6)	8(1)	3.0(8)	3.0	1.5	40.7
3,3,3-LICAMS	41(6)	9(1)	2.8(2)	3.3	1.0	55.9
4,3,4-LICAMS	30(6)	11(2)	3.7(6)	4.3	7.5	56.6
2,3,3,3-CYCAMS	30(7)	18(2)	7(1)	4.7	4.0	61.4
2,3,2-LICAMS	26(3)	13(1)	12(1)	8.1	3.9	63.0
3,3,3,3-CYCAMS	32(4)	14(1)	10(2)	4.7	4.7	64.7
3,3,3,3-CYCAM	23(7)	18(4)	3(1)	3.6	40.9	88.9
3,2,3,2-CYCAM-NO_2	37(8)	8(1)	26(4)	16.3	6.0	92.8
$CaNa_3DTPA$	17(4)	11(1)	3(1)	5.2	0.5	36.7
Desferrioxamine	23(6)	20(2)	4(1)	4.2	1.6	52.2
DiMeCAMS	49(7)	30(7)	7(1)	5.9	1.5	93.6
DBHA[c]	50(5)	31(6)	8(2)	6.7	1.5	96.5
1 hr Control	30(5)	23(2)	32(2)	12.3	3.4	~100
24 hr Control	51(7)	31(6)	5.1(8)	4.6	2.6	93.9

[a]Ligands were administered 1 hour and the mice were killed 24 hours after injection of $^{238}Pu(IV)$ citrate.

[b]Five mice per group except for 4,4,4-LICAMS (10 mice), 1 hour control (7 mice) and 24 hour control (34 mice).

[c]2,3-Dihydroxybenzoic acid.

Table 8. Effect of 3,4,3-LICAMS on Plutonium Retention in Beagles.[a]

	Percent Injected Dose[b]		
	Whole Body	Liver	Non-liver
Control	90	35	55
LICAMS	13.7	6.3	7.4
DTPA	29.7	9.9	19.8
DTPA + LICAMS	11.6	4.9	6.7

[a]Ligands were administered 30 minutes and the dogs were killed 7 days after injection of the radionuclides.

[b]Two dogs per group, except that the control values were taken from references 90-92.

Table 9. Summary of Actinide Sequestering Properties of Tetrameric Catechoylamides.

Cyclic		
3,3,3,3-CYCAM	Mobilizes Pu but deposits it in kidneys	
3,2,3,2-CYCAM-NO_2	Very toxic	
3,3,3,3-CYCAMS, 2,3,3,3-CYCAMS	Sulfonation increases acidity and solubility, prevents Pu deposition in kidneys	
Linear		
2,3,2-LICAMS	Least effective of linear compounds	
3,3,3-LICAMS, 4,3,3-LICAMS	Longer chain length, slight improvement, still not very effective	
4,4,4-LICAMS	Slightly toxic	Longer central bridge gives optimum geometry
3,4,3-LICAMS	Derivative of spermine (a natural product)	

Less constrained linear structures are superior to corresponding cyclic compounds.

Figure Captions

Figure 1. Diethylenetriaminepentaacetic acid (DTPA).

Figure 2. Representative siderophores.

Figure 3. Eight Coordinate polyhedra. The principal axes are vertical. Edge labels are taken from references 43 and 46.

Figure 4. Cyclic voltammogram of $[Ce(O_2C_6H_4)_4]^{4-}$ in 5 M NaOH, 1 M catechol aqueous solution, on a hanging mercury drop electrode, at 100 mV/sec scan rate.

Figure 5. The $[M(catechol)_4]^{4-}$ (M = Hf, Ce, Th, U) anion viewed along the mirror plane with the $\bar{4}$ axis vertical. The dodecahedral A and B sites are shown.

Figure 6. $Th(i\text{-}Pr\text{-}N(O)\text{-}C(O)\text{-}t\text{-}Bu)_4$ viewed down the $\bar{4}$ axis. In this Figure and in Figure 8, the substituent carbon atoms are drawn at 1/5 scale, the hydrogen atoms are omitted for clarity, and the nitrogen and nitrogen oxygen atoms are shaded.

Figure 7. The coordination polyhedron of $Th(i\text{-}Pr\text{-}N(O)\text{-}C(O)\text{-}t\text{-}Bu)_4$ compared to a cube and a dodecahedron.

Figure 8. $Th(i\text{-}Pr\text{-}N(O)\text{-}C(O)\text{-}Neopentyl)_4$ viewed down the pseudo $\bar{4}$ axis.

Figure 9. Schematic structure of $Th(i\text{-}Pr\text{-}N(O)\text{-}C(O)\text{-}Neopentyl)_4$ emphasizing its relationship to a dodecahedron.

Figure 10. Molecular structure of $UO_2Cl(PBHA)(THF)_2$.

Figure 11. Schematic structure of the tetracatechol actinide sequestering agents from a biomimetic approach based on Enterobactin.

Figure 12. Ceneral synthesis and structure of catechoylamides. The cyclic catechoylamides, in which R = $(CH_2)_p$ are abbreviated as n,m,p,m-CYCAM. The sulfonated and the analogous nitro derivatives are indicated by n,m,p,m-CYCAMS and n,m,p,m-CYCAM-NO_2 respectively. The linear sulfonated catechoylamides are abbreviated as m,n,m-LICAMS. A prefix is added to indicate terminal N substituents.

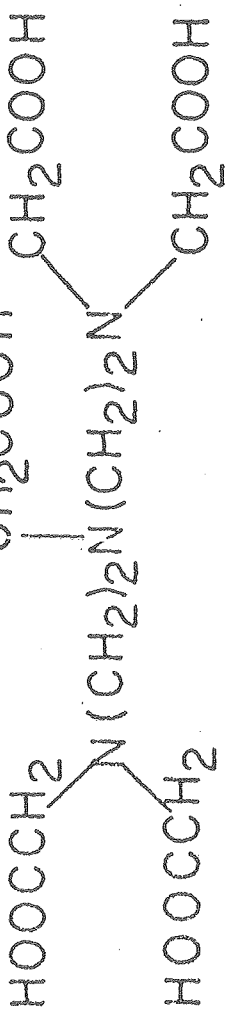

XBL7910-4220

Fig. 1

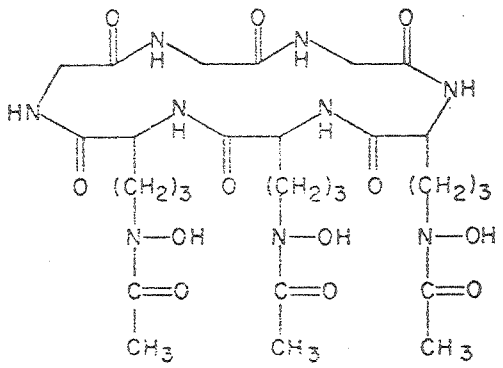

Desferrichrome

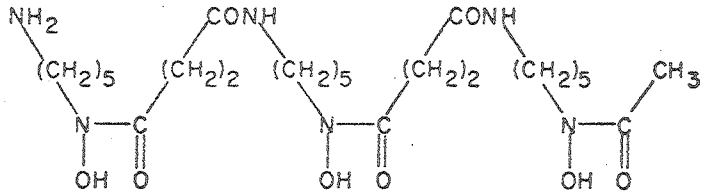

Desferrioxamine B

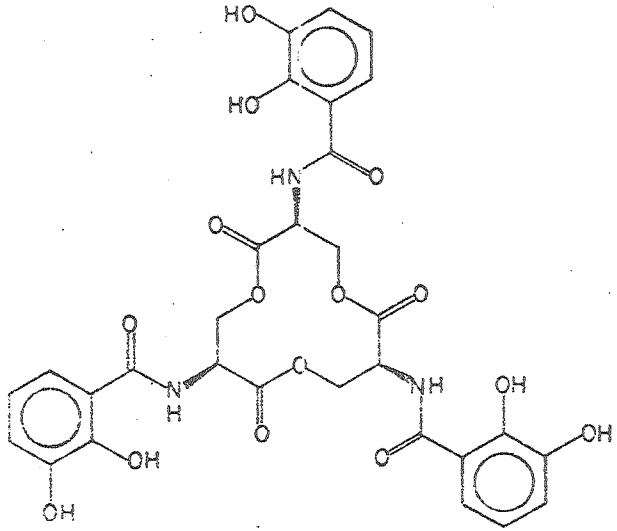

Enterobactin

XBL 7910-4223

Fig. 2

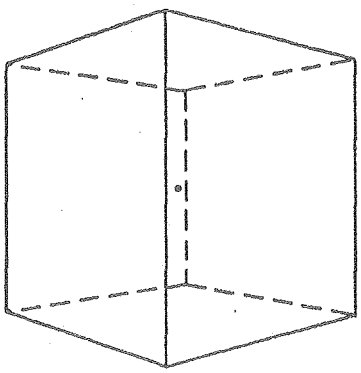

Cube
O_h

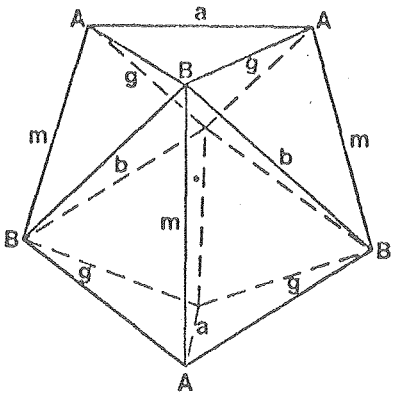

Dodecahedron
D_{2d}

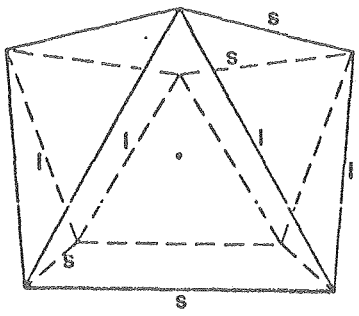

Square Antiprism
D_{4d}

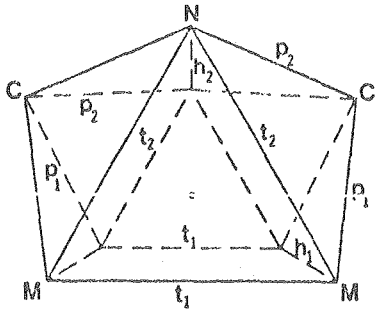

Bicapped Trigonal Prism
C_{2v}

XBL 799-11289

Fig. 3

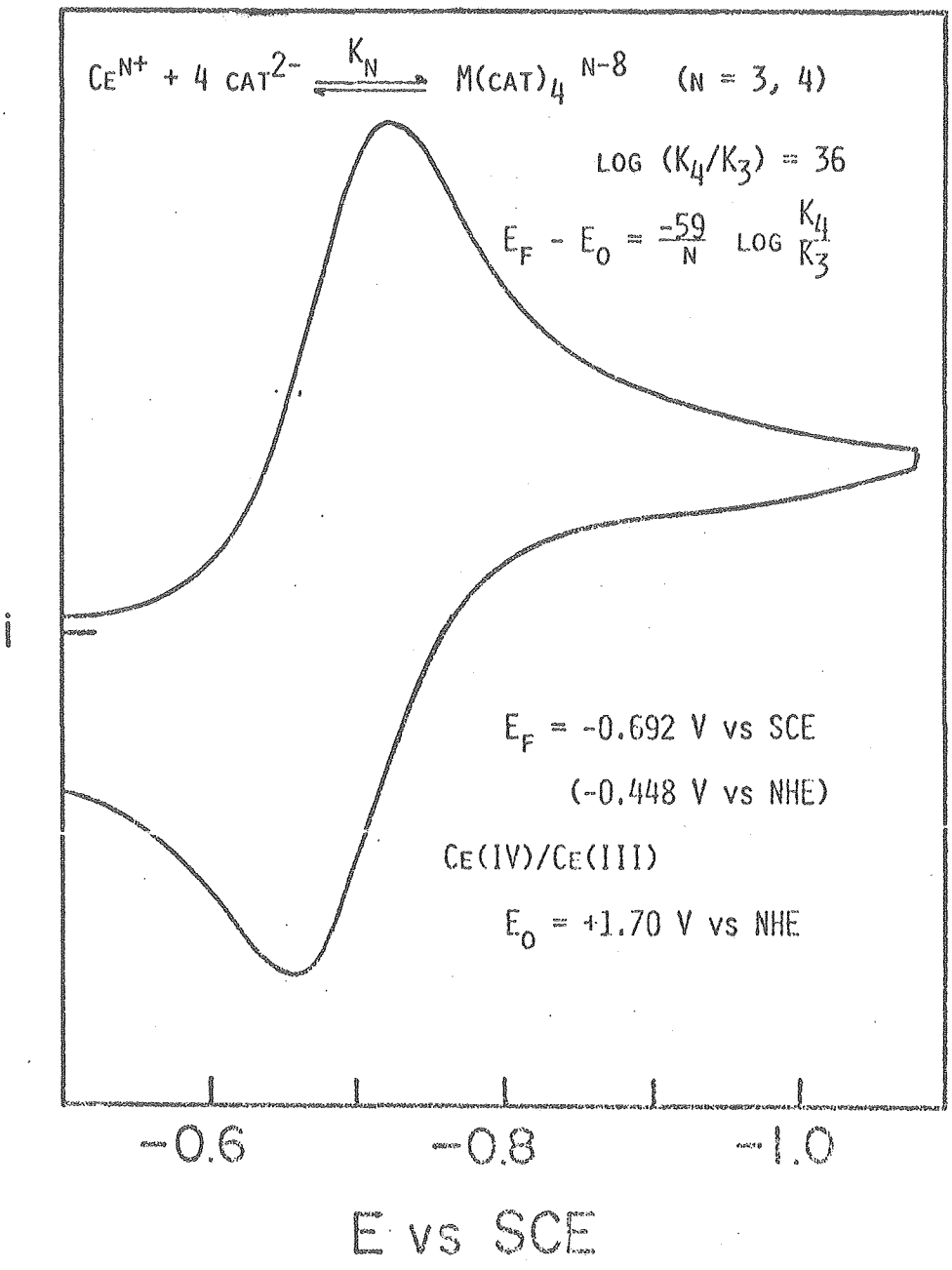

XBL 7810-11691A

Fig. 4

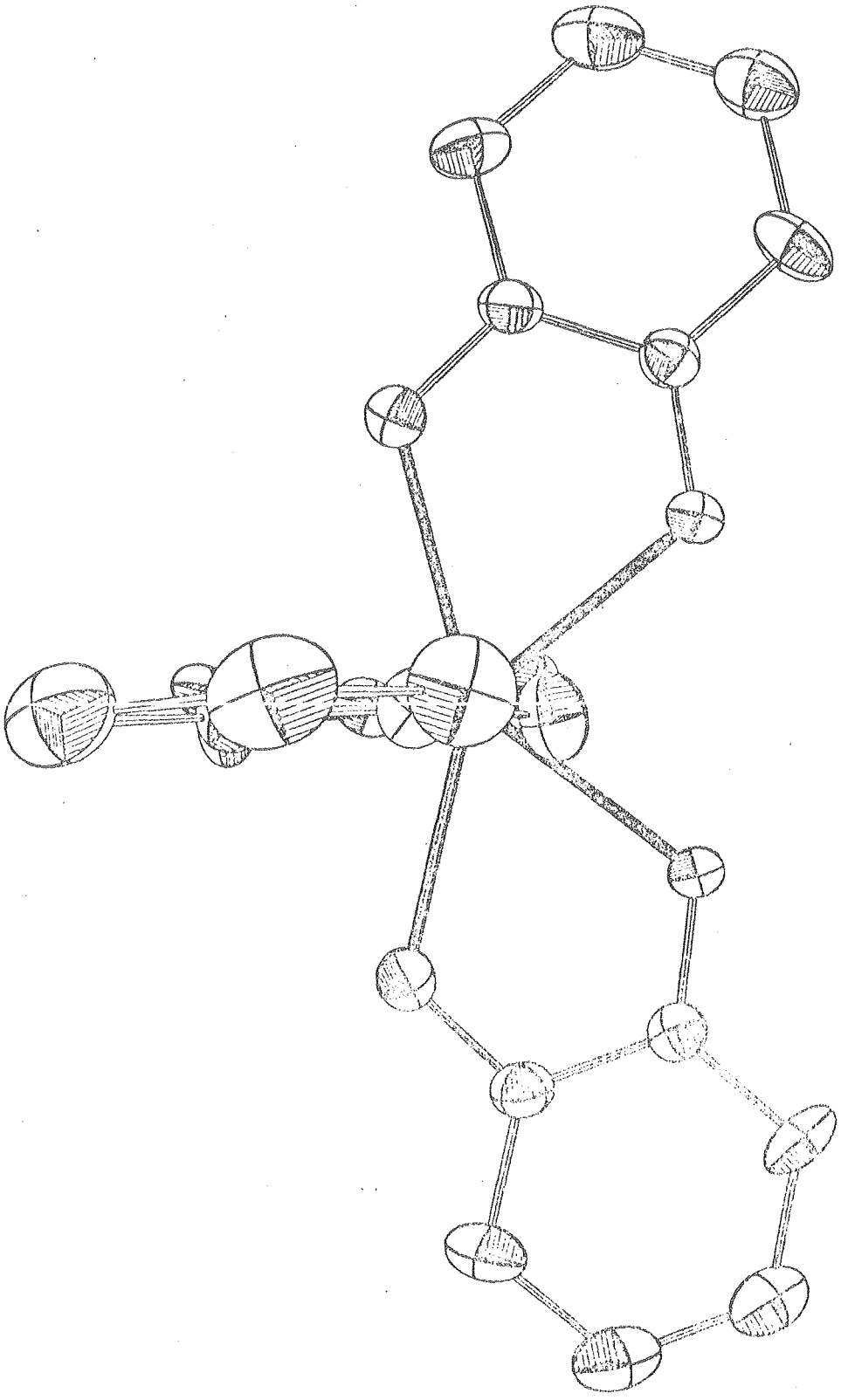

XBL 781-6965

Fig. 5

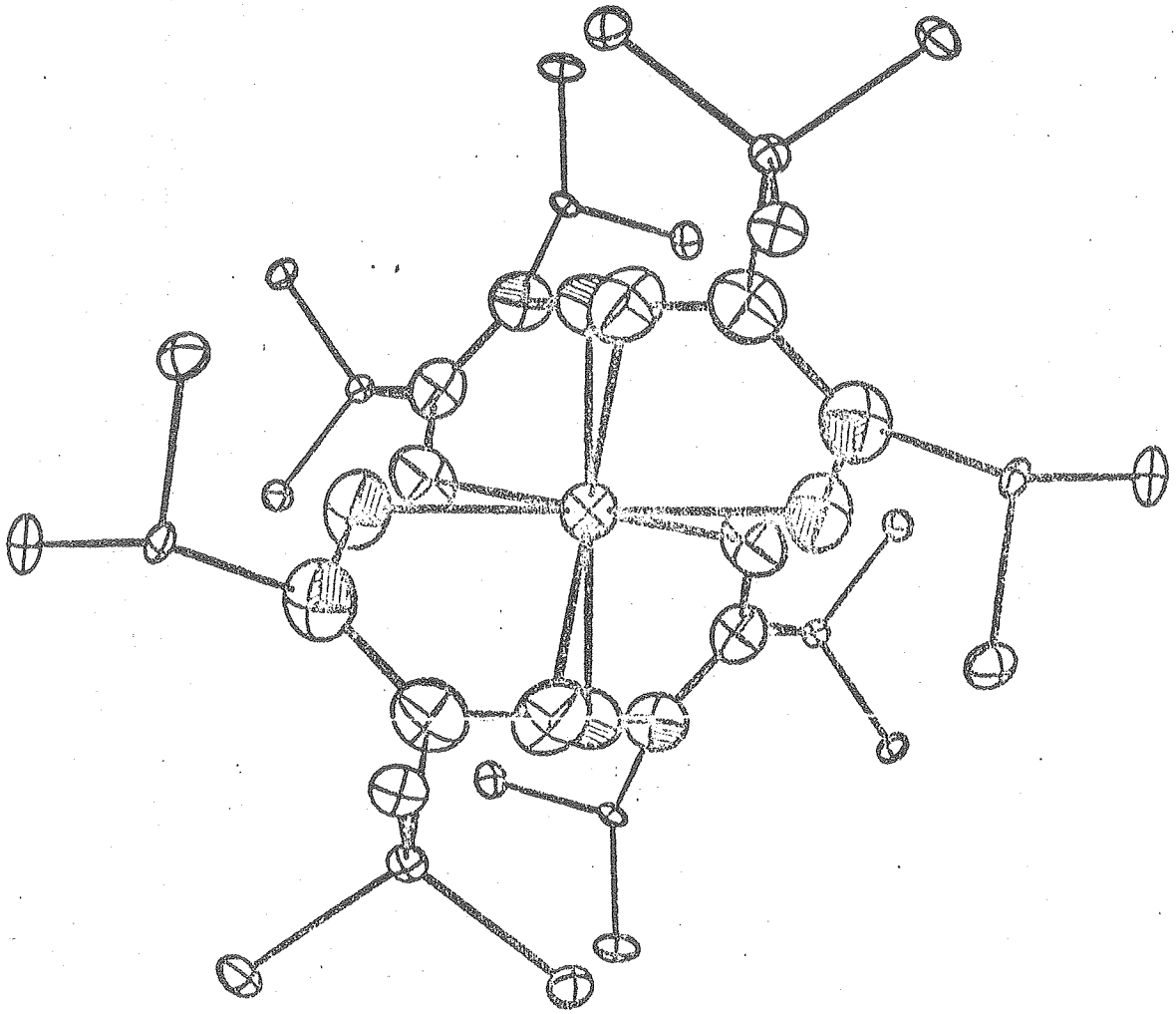

XBL 796-10274

Fig. 6

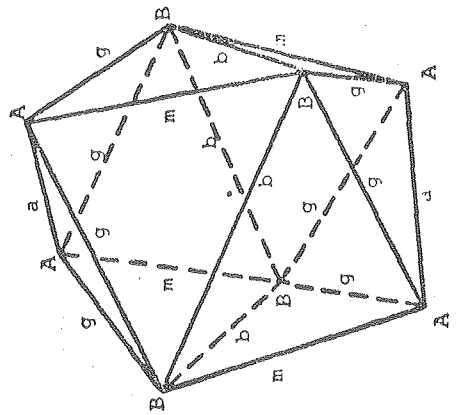

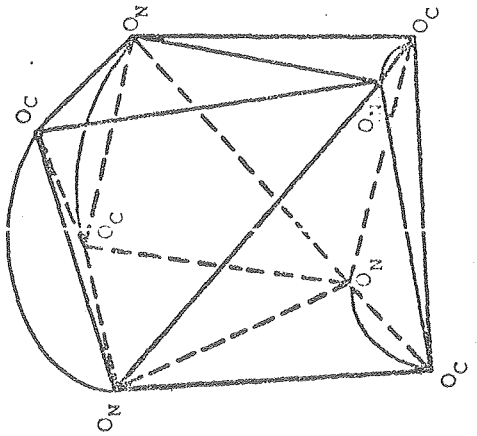

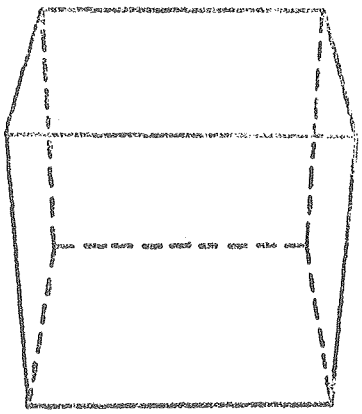

XBL 796-10271

Fig. 7

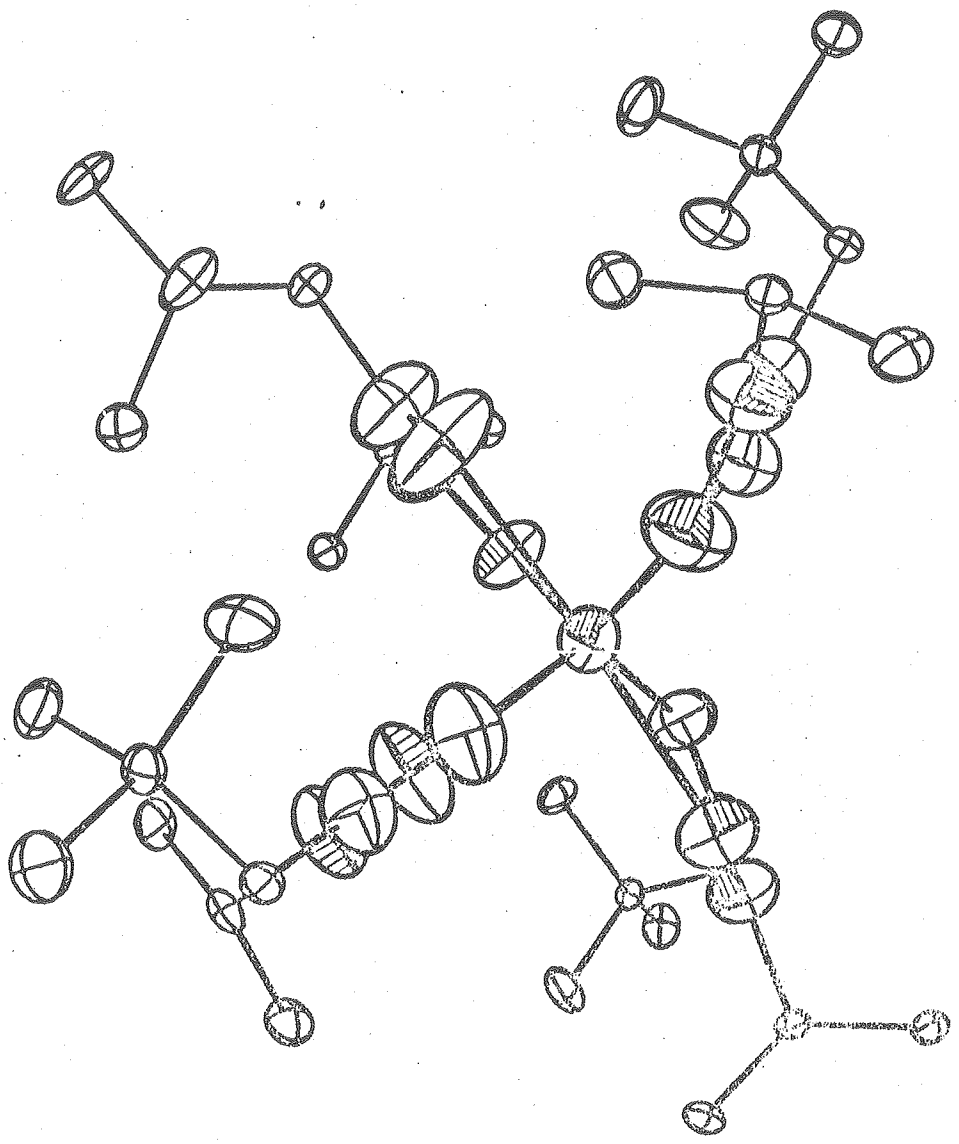

XBL 799-11354

Fig. 8

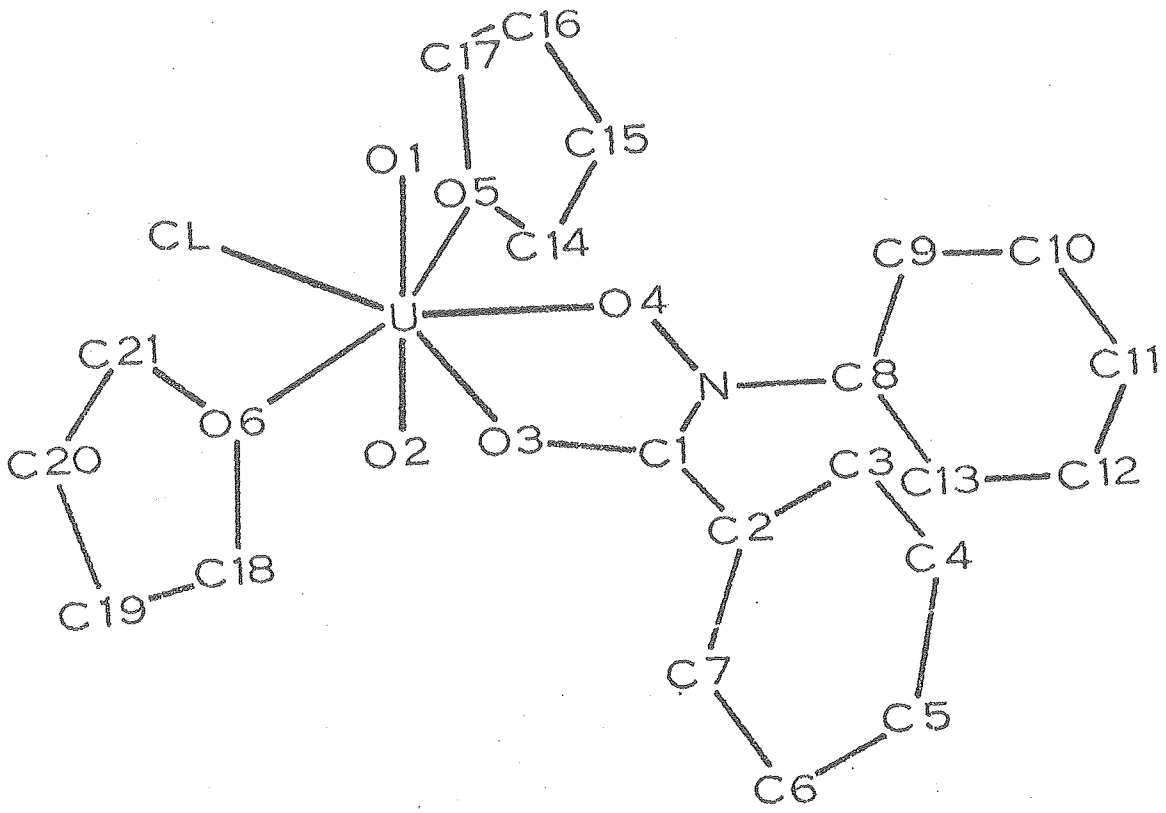

XBL 783-7435

Fig. 9

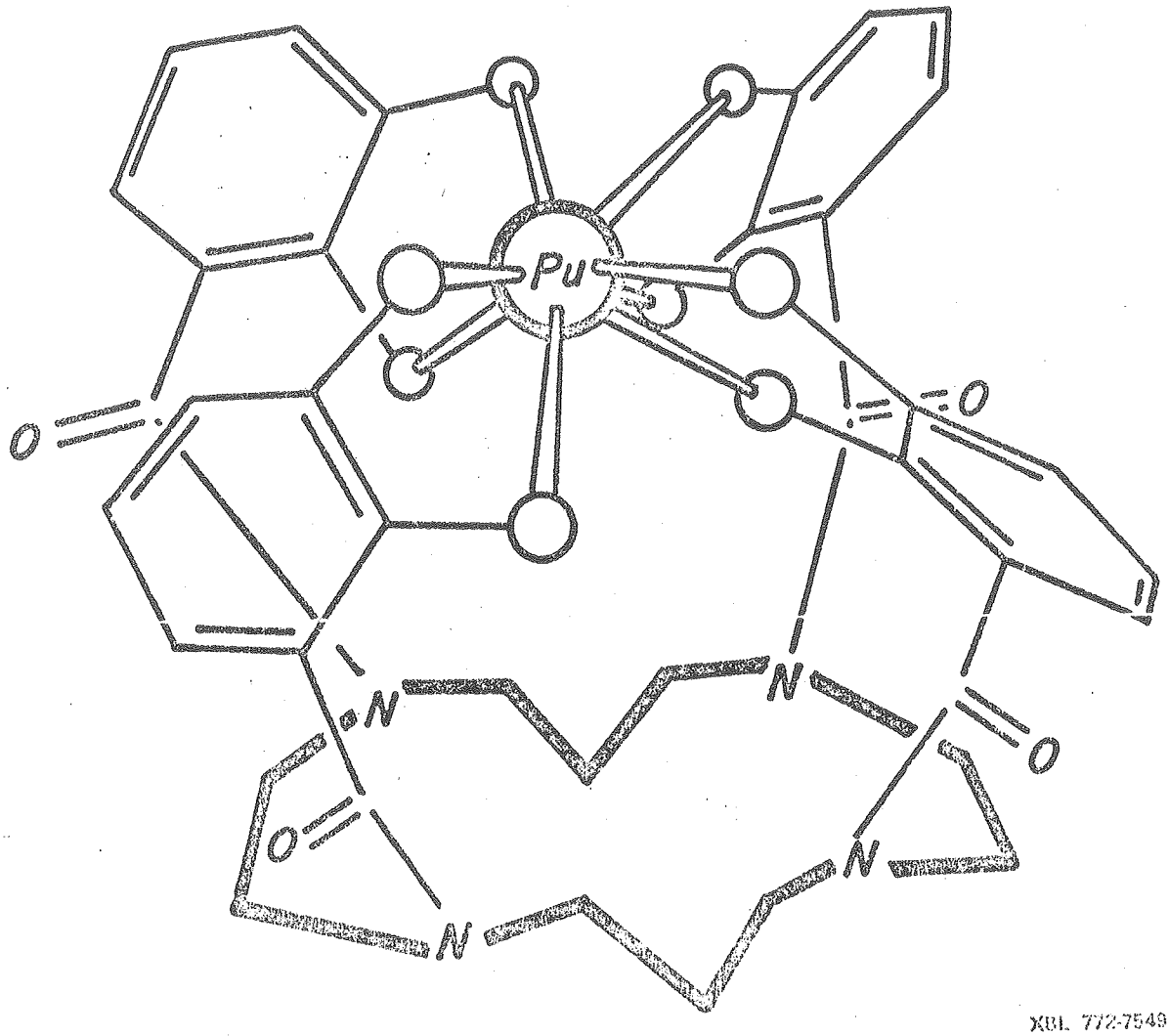

XBL 772-7549

Fig. 10

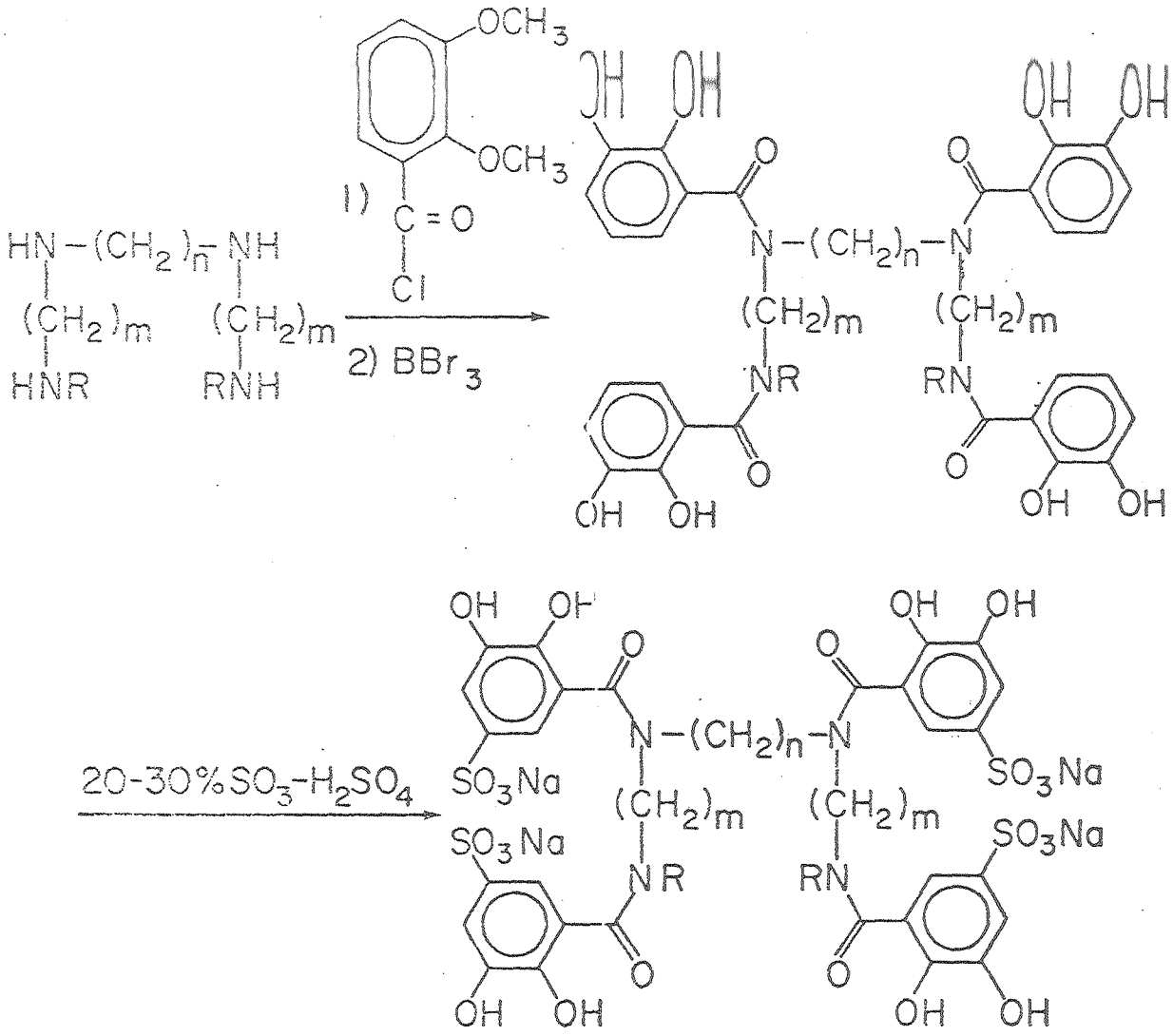

XBL 7910-4417

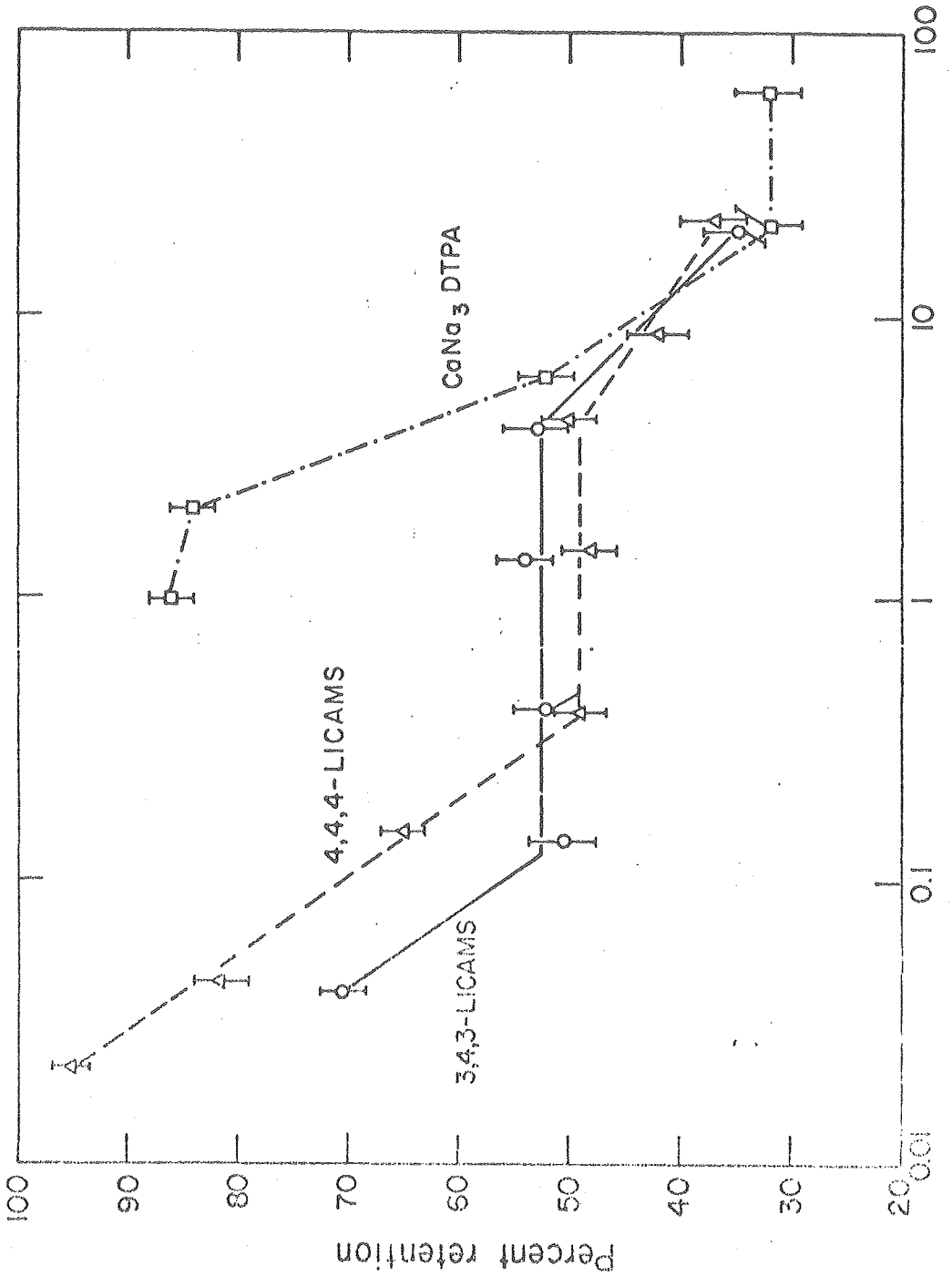
Percent retention
100
90
80
70
60
50
40
30
20
0.01
0.1
1
10
100
Ligand dose μmole/kg
CaNa3 DTPA
4,4,4-LICAMS
3,4,3-LICAMS
XBL 7910-4219

Fig. 12